



HAL
open science

Structural, magnetic and gas sensing properties of nanosized copper ferrite powder synthesized by sol gel combustion technique

Thondiyanoor Pisharam Sumangala, Chegonda Mahender, Antoine Barnabé,
Narayanan Venkataramani, Shiva Prasad

► To cite this version:

Thondiyanoor Pisharam Sumangala, Chegonda Mahender, Antoine Barnabé, Narayanan Venkataramani, Shiva Prasad. Structural, magnetic and gas sensing properties of nanosized copper ferrite powder synthesized by sol gel combustion technique. *Journal of Magnetism and Magnetic Materials*, 2016, 418, pp.48-53. 10.1016/j.jmmm.2016.02.053 . hal-02378851

HAL Id: hal-02378851

<https://hal.science/hal-02378851>

Submitted on 25 Nov 2019

HAL is a multi-disciplinary open access archive for the deposit and dissemination of scientific research documents, whether they are published or not. The documents may come from teaching and research institutions in France or abroad, or from public or private research centers.

L'archive ouverte pluridisciplinaire **HAL**, est destinée au dépôt et à la diffusion de documents scientifiques de niveau recherche, publiés ou non, émanant des établissements d'enseignement et de recherche français ou étrangers, des laboratoires publics ou privés.




Open Archive Toulouse Archive Ouverte (OATAO)

OATAO is an open access repository that collects the work of Toulouse researchers and makes it freely available over the web where possible

This is an author's version published in: <http://oatao.univ-toulouse.fr/25119>

Official URL: <https://doi.org/10.1016/j.jmmm.2016.02.053>

To cite this version:

Sumangala, Thondiyanoor Pisharam and Mahender, Chegonda and Barnabé, Antoine  and Venkataramani, Narayanan and Prasad, Shiva *Structural, magnetic and gas sensing properties of nanosized copper ferrite powder synthesized by sol gel combustion technique*. (2016) *Journal of Magnetism and Magnetic Materials*, 418. 48-53. ISSN 0304-8853

Any correspondence concerning this service should be sent to the repository administrator: tech-oatao@listes-diff.inp-toulouse.fr

Structural, magnetic and gas sensing properties of nanosized copper ferrite powder synthesized by sol gel combustion technique

T.P. Sumangala^a, C. Mahender^a, A. Barnabe^c, N. Venkataramani^a, Shiva Prasad^{b,*}

^a Department of Metallurgical Engineering and Materials Science, Indian Institute of Technology Bombay, Powai, Mumbai 400076, India

^b Department of Physics, Indian Institute of Technology Bombay, Powai, Mumbai 400076, India

^c Université de Toulouse, Institut Carnot CIRIMAT – UMR CNRS-UPS-INP 5085, Université Paul Sabatier, Toulouse 31062, France

ARTICLE INFO

Keywords:

Magnetic materials

Nanostructures

Sol-gel combustion synthesis

X-ray diffraction

In-situ high temperature XRD

Chemical sensing

ABSTRACT

Stoichiometric nano sized copper ferrite particles were synthesized by sol gel combustion technique. They were then calcined at various temperatures ranging from 300 800 °C and were either furnace cooled or quenched in liquid nitrogen. A high magnetisation value of 48.2 emu/g signifying the cubic phase of copper ferrite, was obtained for sample quenched to liquid nitrogen temperature from 800 °C. The ethanol sensing response of the samples was studied and a maximum of 86% response was obtained for 500 ppm ethanol in the case of a furnace cooled sample calcined at 800 °C. The chemical sensing is seen to be correlated with the c/a ratio and is best in the case of tetragonal copper ferrite.

1. Introduction

Recently, spinel ferrites are extensively studied for their potential use as chemical sensors, in their pure form, as mixtures and as spinel ferrite metal oxide composite materials [1–4]. It is also known that many factors such as the chemical species, surface morphology, synthesis methods and operating temperature affects the chemical sensing response. There have been a few reports comparing the chemical sensing response of various ferrites. Rezliescu et al. [5] have compared the response of copper, cadmium and zinc ferrite and have shown that copper ferrite responds more towards reducing gases than the other two. The operating temperature of ferrites varies from 250 °C to 550 °C. It was shown earlier that copper ferrite detects ethanol at lower temperature of 290 °C, in comparison with nickel ferrite (550 °C) [6], magnesium ferrite (335 °C) [7] and cadmium ferrite 380 °C [8].

Among these ferrites, copper ferrite, is a mixed ferrite and is interesting because of its gas sensing and structural properties. The magnetisation values in copper ferrite are quite distinct, ~1700 G (25 emu/g for room temperature measurement of powder samples) for tetragonal and > 3000 G (44 emu/g) for the cubic phase [9,10]. In bulk it has a tetragonally distorted spinel structure when most Cu^{2+} ions occupy the octahedral B site, in

which case this site occupancy also leads to Jahn Teller distortion, rendering the c/a ratio to be > 1 at room temperature. This transforms to the cubic phase above 350 °C. Additionally it is also known, in the case of bulk, that only high temperature quenching (from 1300 °C) results in the cubic phase. Magnetisation enhancement of copper ferrite by stabilizing the cubic phase at room temperature has been reported in thin films [9]. The magnetisation enhancement is possible if Cu^{2+} ions from the octahedral site migrate to the tetrahedral site. This affects both the structure and magnetic properties. Since chemical sensing is normally ion specific, it was surmised that in the case of copper ferrite, thermal treatment may influence the cation site occupancy and thus the sensing performance.

The effect of thermal treatment on the magnetic properties of copper ferrite is well studied [11]. However, the effect of structural changes due to thermal treatments on the gas sensing response is not well studied. All the earlier works on gas sensing of copper ferrite were on the tetragonal phase. In this work, we have chosen sol gel combustion technique for synthesis of the powder samples. Sol gel combustion is a versatile technique (leads to synthesis of nanocrystalline powders and which in turn may cause interesting gas sensing behaviour) and may be scaled to mass production. Recently, there have been many reports on the sol gel combustion technique using different reduction agents and eco friendly approaches [12–14].

In this paper, we study the effect of thermal treatment on the structural, magnetic and chemical sensing properties of copper

* Corresponding author.

E-mail address: shiva.pd@gmail.com (S. Prasad).

ferrite prepared by the sol gel combustion technique.

2. Experimental details

Copper ferrite powder was synthesized by the sol gel combustion technique discussed elsewhere [15]. The obtained powder sample was ball milled using yttria stabilized zirconium balls for 24 hours. The samples were then calcined at temperature ranging from 300 to 800 °C. One part of the powder was cooled slowly in furnace and the other part quenched by introducing it directly from the furnace into liquid nitrogen. The following naming scheme was followed. Sample calcined at 300 °C and cooled in furnace was labelled as CuF300FC where as the quenched one was labelled CuF300QN.

Powder samples were characterised using a Panalytical X Ray diffractometer in the 2θ range 15–80° for a scanning time of 2 h. The XRD of all the samples (except CuF600QN) were recorded on a Bruker D4 machine for characterising the sample further, using Rietveld refinement. Rietveld refinement was performed on all the recorded XRD data using Fullprof software. XRD measurements were also performed at different temperatures on a selected sample using D8 Bruker Advance diffractometer equipped with a 1D LynxEye Detector (Cu K α). XRD spectra were recorded in the temperature range 50–950 °C at intervals of 50 °C. The magnetisation of the samples were measured using a Quantum design physical property measurement system. The $M-H$ loops were recorded with a maximum applied field of 5 T.

The chemical sensing properties of the samples were analysed using a homemade set up. Resistance was measured using Keithley 181 Nanovoltmeter and Keithley 220 Programmable current source. The resistance measurement unit was connected to desk top PC using Labview software. Sensing measurements were performed using ethanol gas (500 ppm) and zero air (synthetic air with N₂ and O₂). It was observed that when ethanol was inserted in the chamber, resistance of the ferrite decreased. When the resistance reached a saturation value the ethanol gas was purged with zero air. The response of the sample was defined as the ratio of the change in resistance in the presence of ethanol to the resistance in air.

3. Results and discussions

3.1. XRD

Fig. 1 shows the room temperature XRD of furnace cooled copper ferrite samples calcined at various temperatures. Sample CuF300FC was compared with JCPDS data card 77 0010 (for cubic copper ferrite).

It was seen that most of the peaks match with cubic copper ferrite. There are some additional peaks, however, which correspond to α -Fe₂O₃ (104) and CuO (111) phases. For samples calcined above 300 °C, it can be seen that peaks (in the XRD measured at room temperature) like (220) starts splitting into two (220) and (202) peaks due to the onset of tetragonality. The splitting of the peaks becomes more apparent with increase in calcination temperature, indicating that tetragonal distortion of the sample increases with calcination temperature.

It is observed that the relative intensity of the additional peaks due to the secondary phases present is not the same in all the samples. The relative intensity of the peaks increases with calcination temperature and is highest for CuF600FC sample. In CuF800FC, the peaks corresponding to α -Fe₂O₃ disappears. However a small peak of CuO is still seen at $\theta=38.8^\circ$. This peak is not clearly visible in the figure, but can be seen after amplifying the intensity.

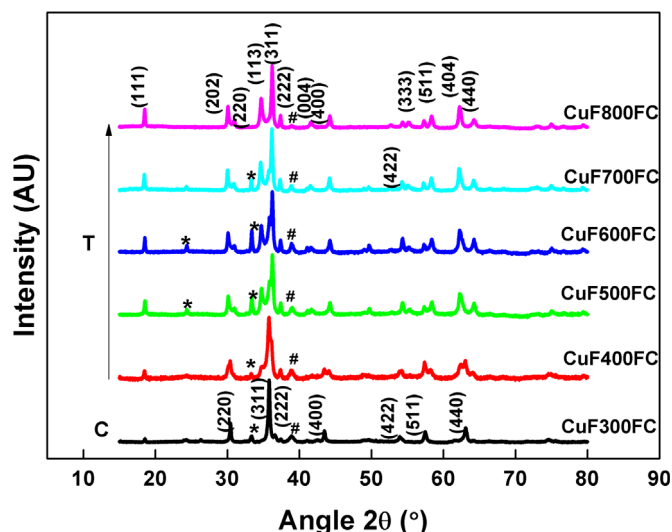


Fig. 1. Room temperature XRD of copper ferrite furnace cooled samples. C and T represent cubic and tetragonal copper ferrite phase respectively. * represents α -Fe₂O₃ phase and # represents CuO phase.

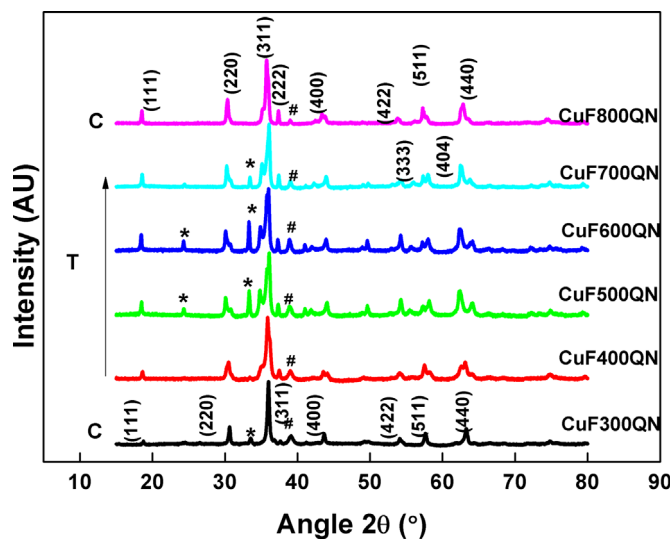


Fig. 2. Room temperature XRD of copper ferrite quenched samples. C and T represent cubic and tetragonal copper ferrite phase respectively. * represents α -Fe₂O₃ phase and # represents CuO phase.

Room temperature XRD of quenched copper ferrite samples, calcined at various temperatures is shown in Fig. 2. The main difference from the XRD of furnace cooled sample is that, in case of quenched samples, copper ferrite moves from a cubic phase to tetragonal phase and reverts back to the cubic phase with increase in calcination temperature.

The volume percent of CuFe₂O₄ present in all samples was calculated from Rietveld refinement and is included in Table 1. From Table 1, it could be seen that the percentage of CuFe₂O₄ shows an initial increase with calcination temperature at 400 °C and falls at 500 and then again increases above 600 °C. The lower content of CuFe₂O₄ in samples calcined at 300 °C may be because the temperature is not sufficient for the formation of spinel phase. However, a further decrease in CuFe₂O₄ content above 400 °C may be due to the precipitation of α -Fe₂O₃ and CuO.

There are several reports in the literature on the presence of impurity phases when CuFe₂O₄ is synthesised in the nanocrystalline powder form [16–19]. The precipitation and disappearance of α -Fe₂O₃ in MgFe₂O₄ was reported earlier [15]. However there is

Table 1
The values of crystallite size, c/a ratio, values of M_∞ and coercivity measured at 5 K and volume percent of CuFe_2O_4 phase for furnace cooled and quenched copper ferrite samples.

Calcination temperature (°C)	Furnace cooled					Quenched				
	Crystallite size (nm)	c/a ratio	M_∞ (emu/g)	Coercivity (Oe)	Volume % of CuFe_2O_4 phase	Crystallite size (nm)	c/a ratio	M_∞ (emu/g)	Coercivity (Oe)	Volume% of CuFe_2O_4 phase
300	20	1.007(5)	41.1	244	79	17	1.004(4)	36.8	241	76
400	24	1.051(5)	33.1	657	92	19	1.047(5)	32.8	577	84
500	26	1.059(3)	21.5	1355	83	23	1.051(2)	26	719	75
600	33	1.060(2)	21	1393	76	24	1.045(5)	28.3	497	67*
700	39	1.060(4)	25.4	1488	89	25	1.043(2)	35	413	82
800	40	1.060(2)	28	1039	95	30	1.009(5)	48.2	348	91

* Gives the value calculated using XRD measured from Panalytical Xray diffractometer.

report on the formation of single phase copper ferrite in the case of RF sputtered thin films (with nanocrystalline grains) deposited using a bulk copper ferrite target [9]. In order to understand whether the appearance of secondary phases are due to the high temperature involved during the synthesis, an Energy Dispersive X Ray Spectroscopy (EDS) was performed on selected samples. The EDS showed that the Fe/Cu ratio was 1.96 ± 0.06 . This shows that the synthesis method has not resulted in volatilisation of Cu.

Crystallite size of all samples was calculated using Scherrer's formula and is given in Table 1. It could be seen from Table 1, that crystallite size of all samples are ≤ 40 nm, which shows the nano crystalline nature of the sample. TEM and SEM were performed on selected samples. The particle size distribution was obtained from them and it was seen to vary from 60 to 120 nm for samples calcined above 600 °C.

Lattice parameter and the c/a ratio were calculated for all the samples from Rietveld refinement. Table 1 shows the values of c/a ratio as a function of calcination temperature. It can be seen from Table 1 that the c/a ratio of furnace cooled sample increases from 1.00 for CuF300FC sample to 1.06 for CuF500FC sample and remains constant thereafter for samples calcined above 500 °C. Thus it could be seen that furnace cooled copper ferrite changes from a predominantly cubic to a predominantly tetragonal structure for calcination temperature ≥ 500 °C.

In case of quenched sample, c/a ratio increases from 1.00 to 1.05 with calcination temperature and then decreases to 1.00 for a sample calcined and quenched from 800 °C. It can be seen that the c/a ratio does not reach a value of 1.06 as in furnace cooled samples. Samples CuF300QN and CuF800QN are in cubic phase. These results indicate that the stability of cubic and tetragonal phase of copper ferrite in nano crystalline form is different from that of bulk.

In literature, different values of c/a ratio ranging from 1.048 to 1.06 have been reported [9,11]. These samples were calcined/annealed at various temperatures and cooled slowly. The trend in c/a ratio of the furnace cooled samples observed by us is different from the one reported by Tailhades et al. [11]. However the trend in c/a ratio of our quenched samples match with that reported by Tailhades et al. and is lower than their values [11].

3.2. In situ high temperature XRD (HXRd)

Fig. 3 gives the HXRd of one of the samples, CuF700FC recorded by varying temperature from 50 to 950 °C, with a step size of 50 °C. From Fig. 3, it could be seen that, copper ferrite exists in the tetragonal phase up to a temperature of 350 °C. However, above this temperature, copper ferrite transforms from the tetragonal phase to the cubic phase. The additional peak of $\alpha\text{-Fe}_2\text{O}_3$ present disappears at a temperature of 800 °C.

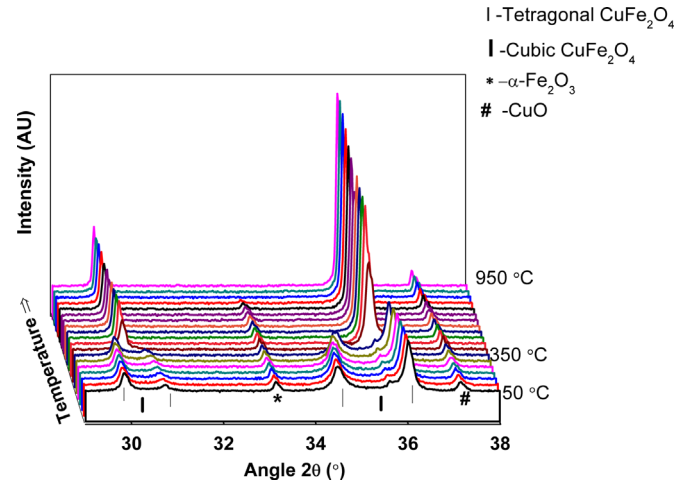


Fig. 3. HXRd of CuF700FC sample measured in-situ at temperatures between 50 and 950 °C with an interval of 50 °C.

3.3. Magnetisation

Magnetic measurements of all the copper ferrite samples were performed at 5 K. Due to the non saturation of the $M-H$ loops, the value of M_∞ was obtained by fitting the high field region to the Eq. (1).

$$M = M_\infty \left(1 - \frac{a}{\sqrt{H}} \right) \quad (1)$$

The details of the method of fitting have been given in an earlier publication [15]. The values of M_∞ obtained by fitting Eq. (1) are given in Table 1, along with the coercivity.

We can see from Table 1, that both M_∞ and coercivity of furnace cooled and quenched samples show non monotonic behaviour with calcination temperature. The value of M_∞ initially decreases, goes through a shallow minimum and then increases. The value of M_∞ is higher in case of quenched samples than the corresponding furnace cooled ones. The non monotonic increase of magnetisation with calcination temperature was already reported for MgFe_2O_4 and was explained on the basis of unequal level of Fe^{3+} ions precipitating from both the sites in the spinel [15].

The measured magnetisation values need to be corrected for additional non magnetic phases. The quantity of additional non magnetic phases present were calculated from Rietveld refinement and the corrected magnetisation values after excluding their masses are shown in Fig. 4. The detail of the mass correction is given in an earlier publication [15]. From Fig. 4, it is seen that the magnetisation of furnace cooled samples decreases continuously whereas the magnetisation of quenched samples initially decreases and then increases above 500 °C.

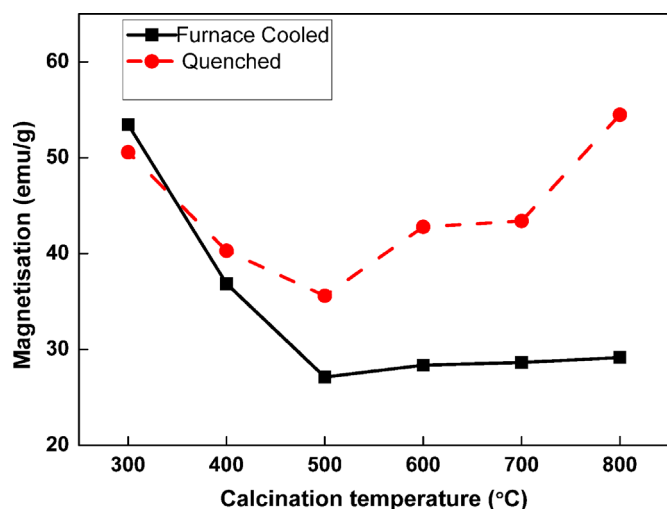


Fig. 4. Magnetisation of furnace cooled and quenched samples after mass correction.

The magnetisation of bulk tetragonal copper ferrite is 30 emu/g (extrapolated to 0 K) [10]. Various values of magnetisation ranging from 34 to 70 emu/g have been reported in literature for nano crystalline system [9,11,20,21]. A maximum value of 48.2 emu/g at 5 K was obtained in our case by quenching from 800 °C. This value is comparable with the literature values (51.5 emu/g by Goya et al. [20] and 52 emu/g by Desai et al. [9]). However, this is smaller than the value reported by Thapa et al., who obtained a magnetization value of 70 emu/g at 5 K by quenching the powder from 1000 °C [21].

From Table 1, it could be seen that the coercivity of the furnace cooled sample initially increases and remains nearly constant above 500 °C (except at 800 °C). In the case of quenched samples the value increases till 500 °C and decreases thereafter. It is also worth noting that the coercivity of the furnace cooled samples above 500 °C is much higher than that of the quenched samples. It was shown earlier that the coercivity of the sample is directly related to the c/a ratio of the sample [11]. In our case also, we observe that the change in coercivity with calcination temperature could be explained in terms of the change in c/a ratio of the samples. Coercivity is higher for samples with high c/a ratio and vice versa.

3.4. Chemical sensing

The response of furnace cooled and quenched copper ferrite samples towards sensing ethanol gaseous vapour was studied. The operating temperature at which a maximum response is obtained was established by systematically varying the operating temperature and measuring the response, to the test gas. The sample CuF800FC with a stoichiometry close to the tetragonal copper ferrite had an operating temperature of 315 °C. This operating temperature was used for recording the sensing response of all other samples. Fig. 5 gives the change in resistance of the one of the samples, CuF800FC with 500 ppm ethanol. It can be seen from the figure that the resistance decreases with the insertion of ethanol into the sensing chamber. The resistance goes back to the initial value after stopping the flow of ethanol gas and re introduction of zero air.

Table 2 gives the response, response time and recovery time of both furnace cooled and quenched samples as a function of calcination temperature at an operating temperature of 315 °C. Samples CuF300FC and CuF300QN do not respond to ethanol and hence have not been included in the Table 2. From the Table 2, it

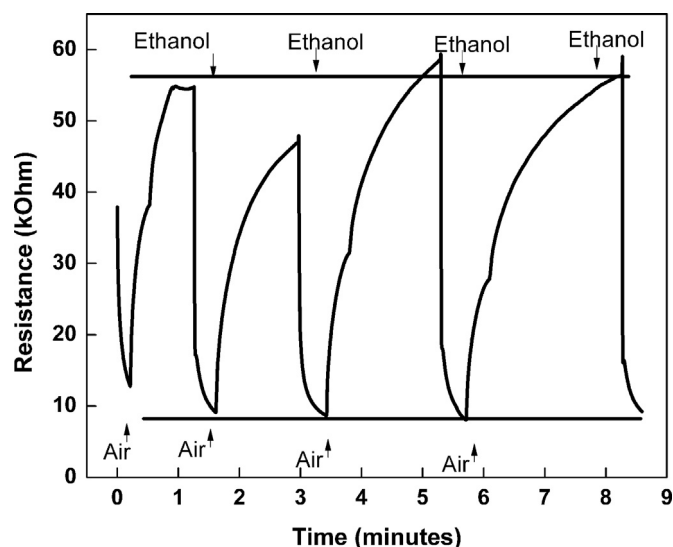


Fig. 5. Change in resistance of CuF800FC sample with 500 ppm ethanol.

can be seen that the response of both furnace cooled and quenched samples decreases initially and then increases with increase in calcination temperature. The response time varied from 3 to 20 min and recovery time varied from 11 to 110 min.

3.5. Discussion

Copper ferrite is tetragonally distorted at room temperature due to the Jahn Teller distortion [22]. The Jahn Teller distortion acts upon the Cu^{2+} ions on the octahedral site. Thus the c/a ratio in this case may vary from 1.04 to 1.06 [11]. At temperatures in the range 250–300 °C, Cu^{2+} ions start migrating from tetrahedral sites to octahedral sites and reverts back at still higher temperature [11].

The migration of Cu^{2+} ions has an impact on the magnetisation of the samples. As the magnetisation in copper ferrite follows Néel's model, the presence of more copper ions on the tetrahedral site leads to an increase in the magnetisation. Thus samples with lower c/a ratio (cubic structure) have higher magnetisation compared to samples with higher c/a ratio (tetragonal structure). This holds true in our case (as can be seen from Fig. 4 and Table 1).

From the ethanol sensing measurements on copper ferrite FC and QN samples, given in Table 2, it can be seen that the response followed a non monotonic rise with calcination temperature. Franke et al. have demonstrated that a decrease in the size of particles in the sensor element results in an improved sensing performance [23]. In our samples, a monotonic increase in crystallite size is seen with calcination temperature. This in turn should have reduced the response of the sensor. However the behaviour of our samples is in contrast to that reported by Franke et al.

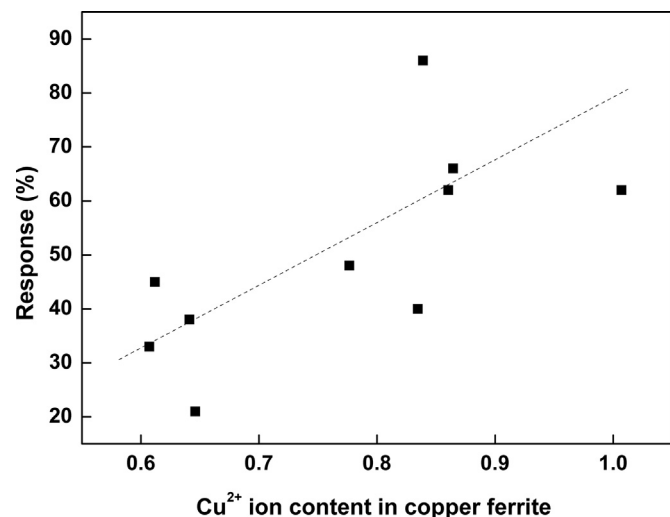
From Figs. 1 and 2, it was seen that additional phases are present in the sample in varying amounts. This implies that the Cu^{2+} ion content in the spinel is not constant in our samples. The total Cu^{2+} ion content in the spinel was calculated using the estimated quantity of each phase obtained using Rietveld refinement. We have plotted the response as a function of Cu^{2+} ion content in the spinel. This is shown in Fig. 6.

From Fig. 6, it can be seen that the response increases with the Cu^{2+} content in the spinel. The increase in Cu^{2+} ion in the spinel lattice corresponds to a decrease in the precipitated amount of CuO in that sample. There have been reports on the improvement in gas sensing response of CuFe_2O_4 with the addition of CuO to the ferrite in the case of weakly reactive gases like CO_2 . It was reported

Table 2

Response, response time and recovery time of both furnace cooled and quenched samples.

Calcination Temperature (°C)	Furnace cooled sample			Quenched sample		
	Response (%)	Response time (min)	Recovery time (min)	Response (%)	Response time (min)	Recovery time (min)
400	48	3	11	33	6	20
500	45	10	12	21	20	60
600	38	7	20	40	13	57
700	62	4	45	62	9	30
800	86	7	110	66	7	100

**Fig. 6.** Response of CuFe_2O_4 sample as a function of Cu^{2+} ion content in the spinel estimated from Rietveld analysis.

that the presence of CuO, (a p type semiconductor (band gap of 1.4–1.9 eV) [24,25]) in contact with copper ferrite (an n type semiconductor) helps in increasing the response by the formation of a p–n junction [1]. However, in our case, the response decreased with the precipitation of CuO.

The decrease in response, as CuO precipitates out from the system may be due to a system deficient in Cu^{2+} ions. This implies that, though the addition of CuO to spinel may improve the response towards certain gases (like CO_2), the response is actually dependent on the total amount of Cu^{2+} ions in the compound. In order to obtain a better response for sensing ethanol, it is observed that either stoichiometric copper ferrite or copper ferrite with excess Cu^{2+} ion content is required. Singh et al. [26] have reported a change in response towards LPG when copper ferrite sample was prepared in Cu/Fe ratios of 1:1, 1:2, 1:3 and 1:4. They found that the response decreased with the increase in Fe content. This is in agreement with our observation that spinel with more Cu^{2+} ions in the structure improve the sensor response.

From Table 2, it could be seen that the response of furnace cooled samples (which are having lower magnetisation than corresponding quenched samples, Table 1) are higher than that of quenched samples. In addition to this, it could be seen that the sample CuF800FC which is in tetragonal phase shows better response than CuF800QN which is in cubic phase. This shows that though cubic phase yields better magnetisation, the response is lower than the corresponding tetragonal phase.

Our study is first one of its kind on the gas sensing performance of cubic copper ferrite. All the earlier works on the gas sensing of copper ferrite was on tetragonal copper ferrite. We have obtained a response of 86% for 500 ppm ethanol using CuF800FC sample. A maximum response of 87% is however reported for 1000 ppm of ethanol, using tetragonal copper ferrite [2,3]. Our studies show

that the response of furnace cooled samples was greater than that of quenched samples and was independent of the c/a ratio. In the case of quenched samples, the response was higher for samples with a higher c/a ratio. From our studies we observe that the presence of second phase alone may not improve the sensing performance. The sensing response of copper ferrite could be enhanced through incorporating excess Cu^{2+} ions into the structure.

4. Conclusions

Nanocrystalline copper ferrite was prepared by sol gel combustion technique. The obtained powder was calcined in the temperature range 300–800 °C and was either furnace cooled or quenched. The XRD of the samples revealed predominant presence of copper ferrite phase. A small quantity of additional phases of CuO and $\alpha\text{-Fe}_2\text{O}_3$ phases were seen in most of the samples. XRD of the furnace cooled samples showed a transition from cubic to tetragonal phase with the rise in calcination temperature. In the case of quenched samples, transition from the cubic to tetragonal phase and back to cubic phase was observed. The cubic to tetragonal phase transition at a temperature of 350 °C was established by recording a variable temperature XRD on a sample in the range 50–950 °C. The precipitation of $\alpha\text{-Fe}_2\text{O}_3$ phase and its disappearance at 800 °C was also observed in the same experiment. Magnetic measurements performed on the samples showed a non monotonic increase with calcination temperature. A maximum value of 48.2 emu/g was obtained for CuF800QN sample. The change in resistance with ethanol vapour was recorded for all the samples. The response of the samples increased non monotonically with calcination temperature and has been correlated to the quantity of Cu^{2+} ions in the spinel structure. A response of 86% was obtained towards 500 ppm ethanol which is comparable with the value of 87% obtained using stoichiometric copper ferrite for 1000 ppm ethanol.

Acknowledgement

Authors thank Central facility IIT Bombay for the Physical Property Measurement Facility (PPMS). Authors thank MonaSens Project DST (grant number 14IFCPAR001) ANR (grant number 13 IS08 0002 01) for funding this study.

Appendix A. Supplementary material

Supplementary data associated with this article can be found in the online version at <http://dx.doi.org/10.1016/j.jmmm.2016.02.053>.

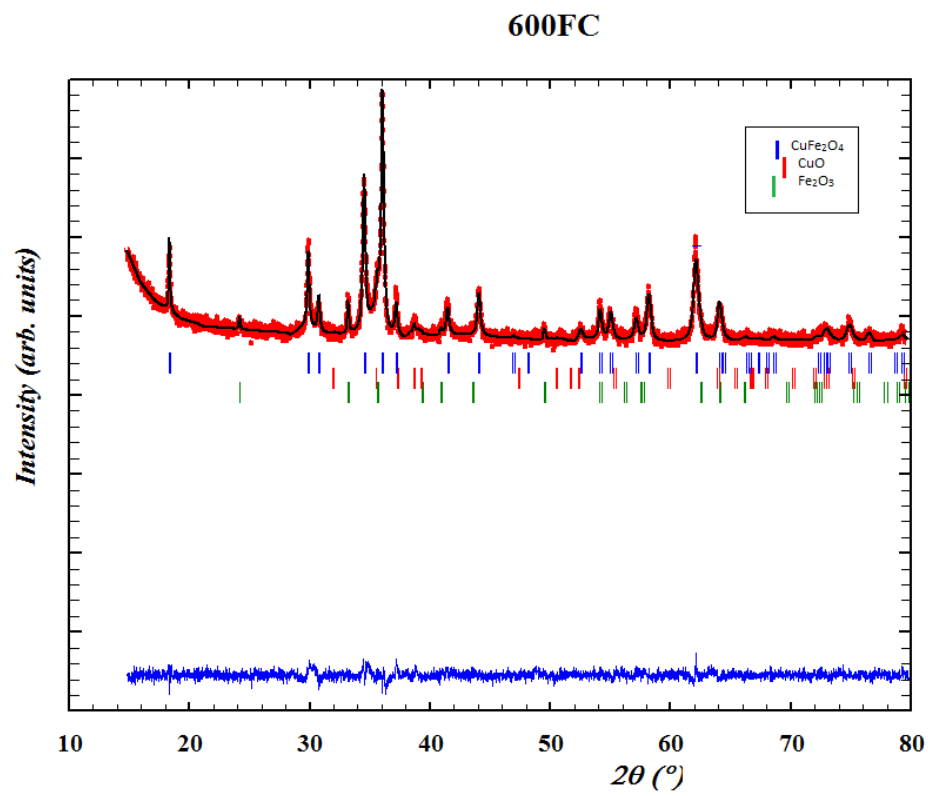
References

- [1] A. Chapelle, F.O. Hassani, L. Presmanes, A. Barnabé, P. Tailhades, CO_2 sensing properties of semiconducting copper oxide and spinel ferrite nanocomposite

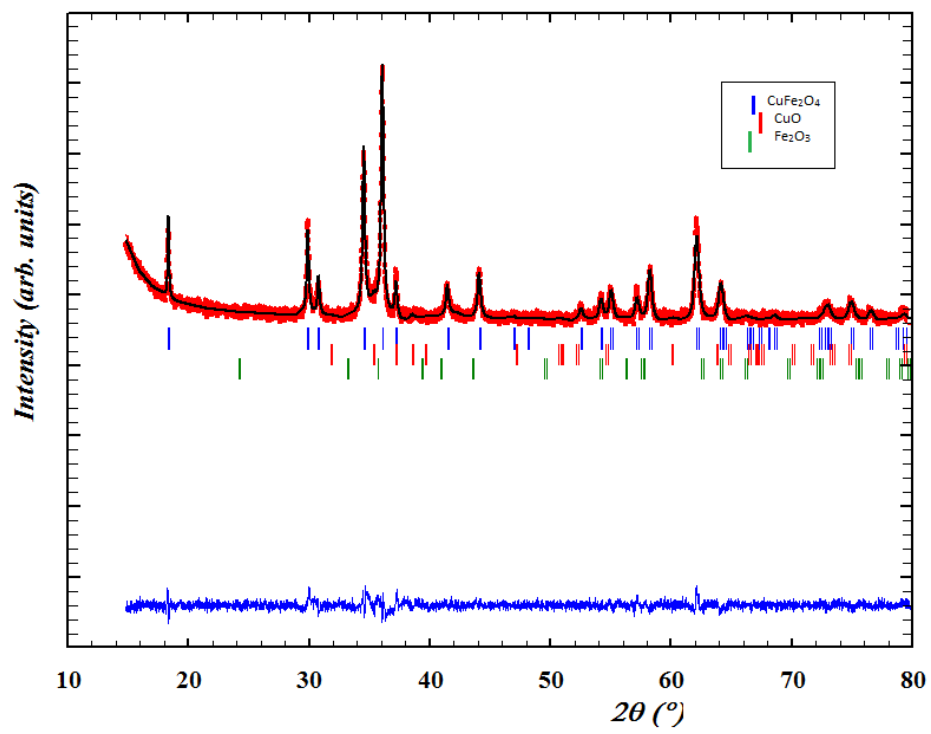
- thin film, *Appl. Surf. Sci.* 256 (2010) 4715–4719.
- [2] Z. Sun, L. Liu, D.Z. Jia, W. Pan, Simple synthesis of CuFe_2O_4 nanoparticles as gas sensing materials, *Sens. Actuators B* 125 (2007) 144–148.
 - [3] S. Tao, F. Gao, X. Liu, O.T. Sørensen, Preparation and gas-sensing properties of CuFe_2O_4 at reduced Temperature, *Mater. Sci. Eng. B* 77 (2000) 172–176.
 - [4] L. Satyanarayana, K.M. Reddy, S.V. Manorama, Synthesis of nanocrystalline $\text{Ni}_{1-x}\text{Co}_x\text{Mn}_x\text{Fe}_{2-x}\text{O}_4$: a material for liquefied petroleum gas sensing, *Sens. Actuators B* 89 (2003) 62–67.
 - [5] N. Rezliescu, E. Rezliescu, F. Tudorache, P.D. Popa, Gas sensing properties of porous Cu, Cd- and Zn- ferrites, *Romanian Rep. Phys.* 61 (2009) 223–234.
 - [6] T. Sathiwitayakul, E. Newton, I.P. Parkin, M. Kuznetsov, R. Binions, Ferrite materials produced from self-propagating high-temperature synthesis for gas sensing applications, *IEEE Sens. J.* 15 (2015) 196–200.
 - [7] Y.L. Liu, Z.M. Liu, Y. Yang, H.F. Yang, G.L. Shen, R.Q. Yu, Simple synthesis of MgFe_2O_4 nanoparticles as gas sensing materials, *Sens. Actuators B* 107 (2005) 600–604.
 - [8] Z. Tianshu, P. Hing, Z. Jiancheng, K. Lingbing, Ethanol-sensing characteristics of cadmium ferrite prepared by chemical coprecipitation, *Mater. Chem. Phys.* 61 (1999) 192–198.
 - [9] M. Desai, S. Prasad, N. Venkataramani, I. Samajdar, A.K. Nigam, R. Krishnan, Annealing induced structural change in sputter deposited copper ferrite thin films and its impact on magnetic properties, *J. App. Phys.* 91 (2002) 2220.
 - [10] J. Smit, H.P.J. Wijn, *Ferrites: Physical Properties of Ferrimagnetic Oxides in Relation to Their Technical Applications*, N.V. Philips, Eindhoven, 1959.
 - [11] Ph Tailhades, C. Villette, A. Rousset, G.U. Kulkarni, K.R. Kannan, C.N.R. Rao, M. Lenglet, Cation migration and coercivity in mixed copper–cobalt spinel ferrite powders, *J. Solid State Chem.* 141 (1998) 56–63.
 - [12] F. Ansari, A. Sobhani, M.S. Niasari, Facile synthesis, characterization and magnetic property of $\text{CuFe}_{12}\text{O}_{19}$ nanostructures via a sol–gel auto-combustion process, *J. Magn. Magn. Mater.* 401 (2016) 362–369.
 - [13] F. Ansari, A. Sobhani, M.S. Niasari, $\text{PbTiO}_3/\text{PbFe}_{12}\text{O}_{19}$ nanocomposites: Green synthesis through an eco-friendly approach, *Compos. Part B* 85 (2016) 170–175.
 - [14] F. Ansari, A. Sobhani, M.S. Niasari, Sol–gel auto-combustion synthesis of $\text{PbFe}_{12}\text{O}_{19}$ using maltose as a novel reductant, *RSC Adv.* 4 (2014) 63946–63950.
 - [15] T.P. Sumangala, C. Mahender, N. Venkataramani, Shiva Prasad, A study of nanosized magnesium ferrite particles with high magnetic moment, *J. Magn. Magn. Mater.* 382 (2015) 225–232.
 - [16] E. Manova, T. Tsoncheva, D. Paneva, M. Popova, N. Velinov, B. Kunev, K. Tenchev, Ivan Mitov, Nanosized copper ferrite materials: mechanochemical synthesis and characterization, *J. Solid State Chem.* 184 (2011) 1153–1158.
 - [17] N.M. Deraz, Size and crystallinity-dependent magnetic properties of copper ferrite nano-particles, *J. Alloy. Compd.* 501 (2010) 317–325.
 - [18] W. Lv, B. Liu, Z. Luo, X. Ren, P. Zhang, XRD studies on the nanosized copper ferrite powders synthesized by sonochemical method, *J. Alloys Compd.* 465 (2008) 261–264.
 - [19] W. Ponhan, S. Maensiri, Fabrication and magnetic properties of electrospun copper ferrite (CuFe_2O_4) Nanofibers, *Solid State Sci.* 11 (2009) 479–484.
 - [20] G.F. Goya, H.R. Rechenberg, J.Z. Jiang, Structural and magnetic properties of ball milled copper ferrite, *J. Appl. Phys.* 84 (1998) 1101.
 - [21] D. Thapa, N. Kulkarni, S.N. Mishra, P.L. Paulose, P. Ayyub, Enhanced magnetization in cubic ferrimagnetic CuFe_2O_4 nanoparticles synthesized from a citrate precursor: the role of Fe^{2+} , *J. Phys. D: Appl. Phys.* 43 (2010) 195004.
 - [22] H.A. Jahn, E. Teller, Stability of polyatomic molecules in degenerate electronic states I- orbital degeneracy, *Proc. R. Soc. Lond.* 161 (1937) 220–235.
 - [23] M.E. Franke, T.J. Koplin, U. Simon, Metal and metal oxide nanoparticles in chemiresistors: does the nanoscale matter? *Small* 2 (2006) 36–50.
 - [24] S.C. Ray, Preparation of copper oxide thin film by the sol-gel-like dip technique and study of their structural and optical properties, *Sol. Energ. Mat. Sol. Cells* 68 (2001) 307–312.
 - [25] J. Ghijsen, L.H. Tjeng, J. van Elp, H. Eskes, J. Westerink, G.A. Sawatzky, Electronic structure of Cu_2O and CuO , *Phys. Rev. B* 38 (1998) 11322–11330.
 - [26] S. Singh, B.C. Yadav, R. Prakash, B. Bajaj, J.R. Lee, Synthesis of nanorods and mixed shaped copper ferrite and their applications as liquefied petroleum gas sensor, *Appl. Surf. Sci.* 257 (2011) 10763–10770.

Supplementary information

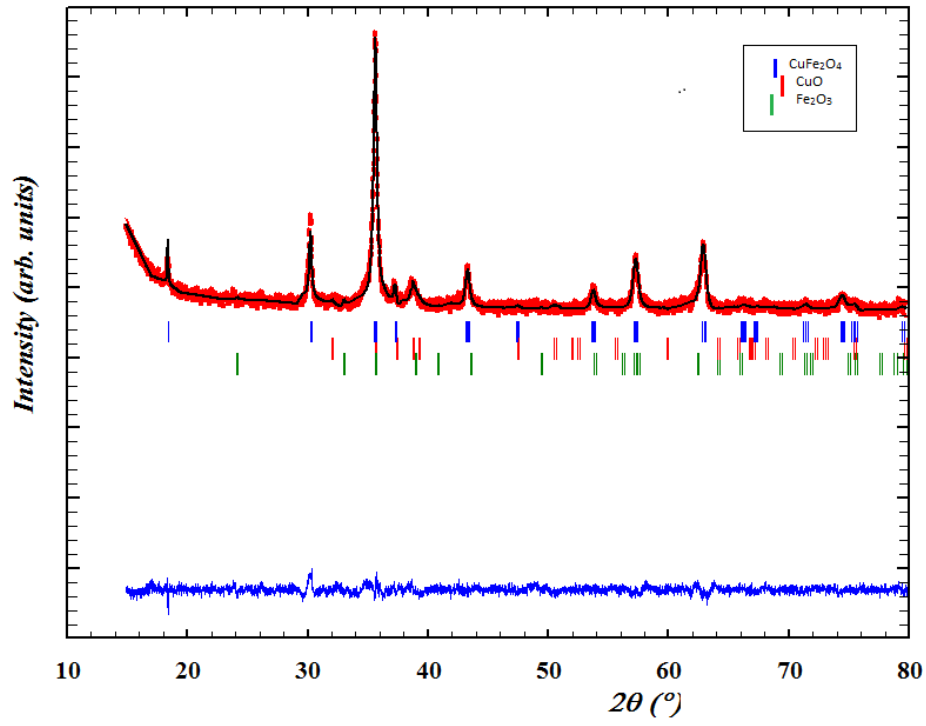
1. Plot of Rietveld refinement of representative samples



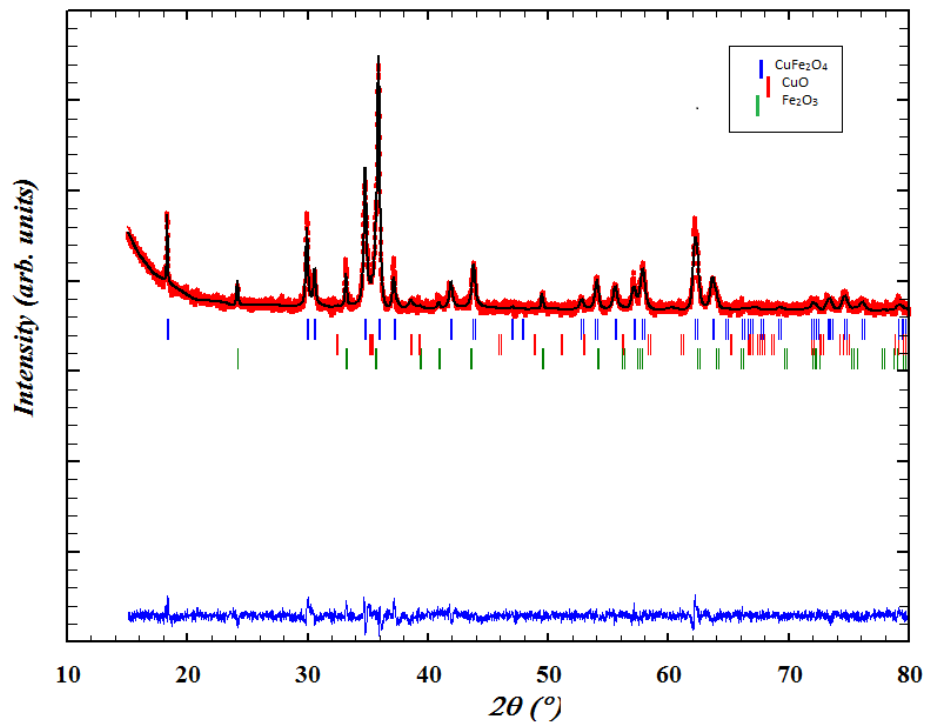
800FC



300QN



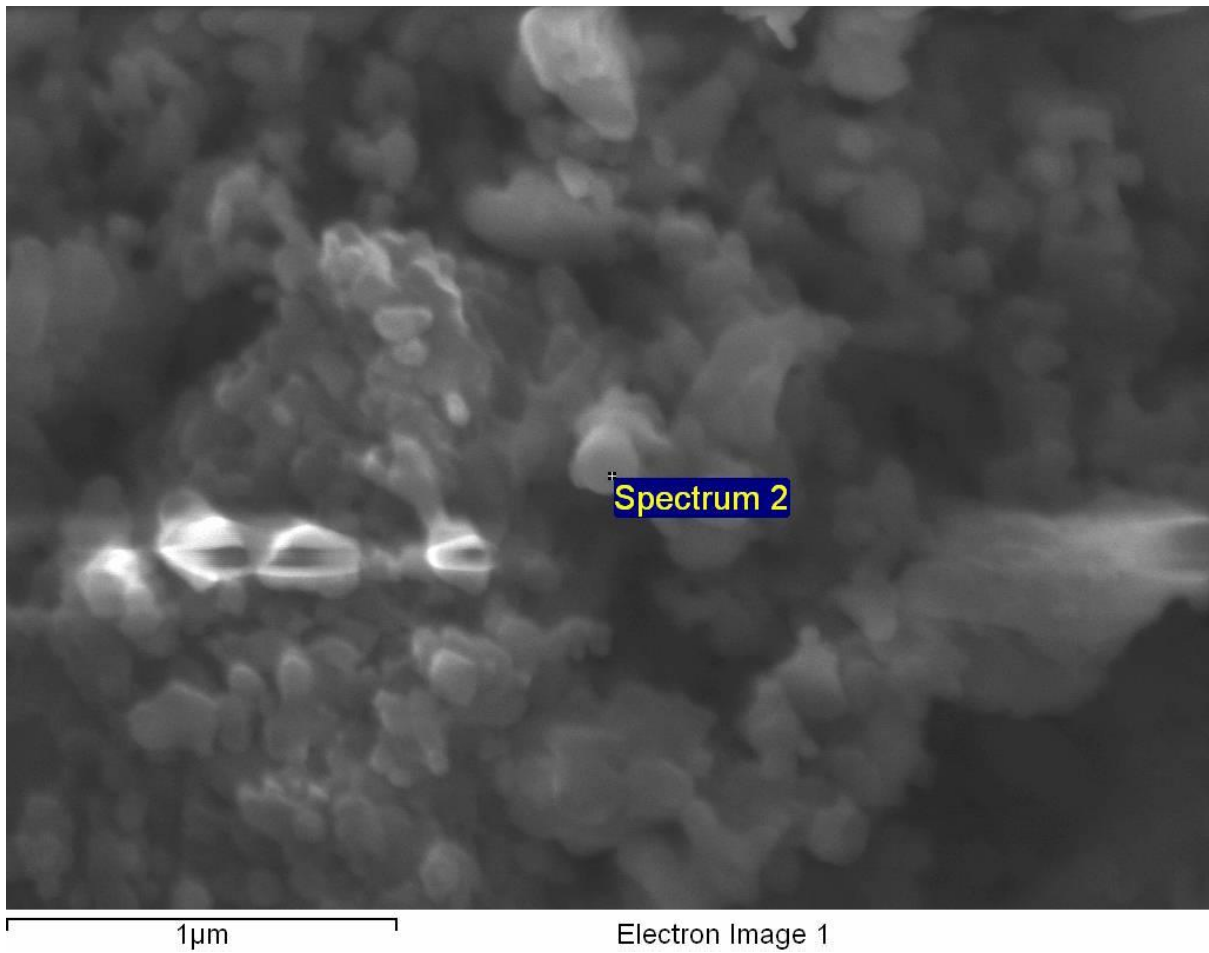
700QN



2. Energy Dispersive X-ray spectroscopy images

Sample: CuF600FC

Area chosen



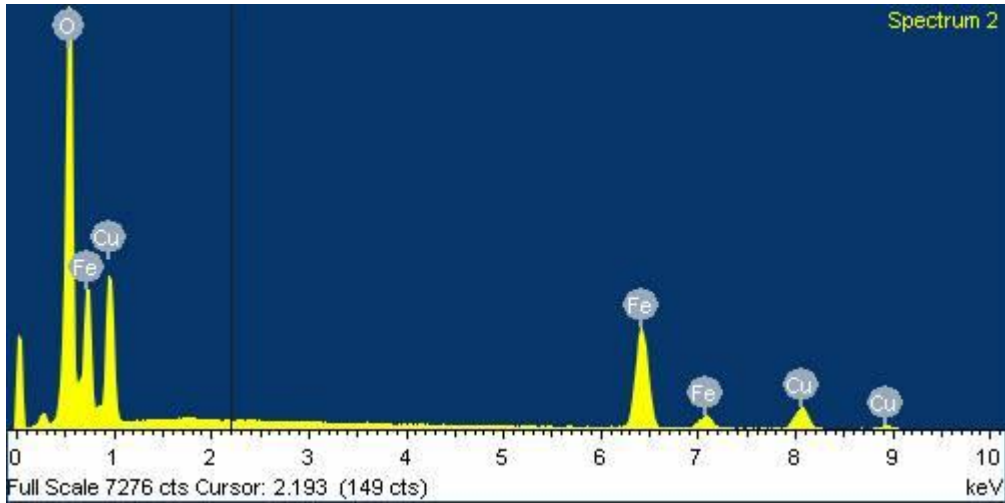
Standard :

O SiO2 1-Jun-1999 12:00 AM

Fe Fe 1-Jun-1999 12:00 AM

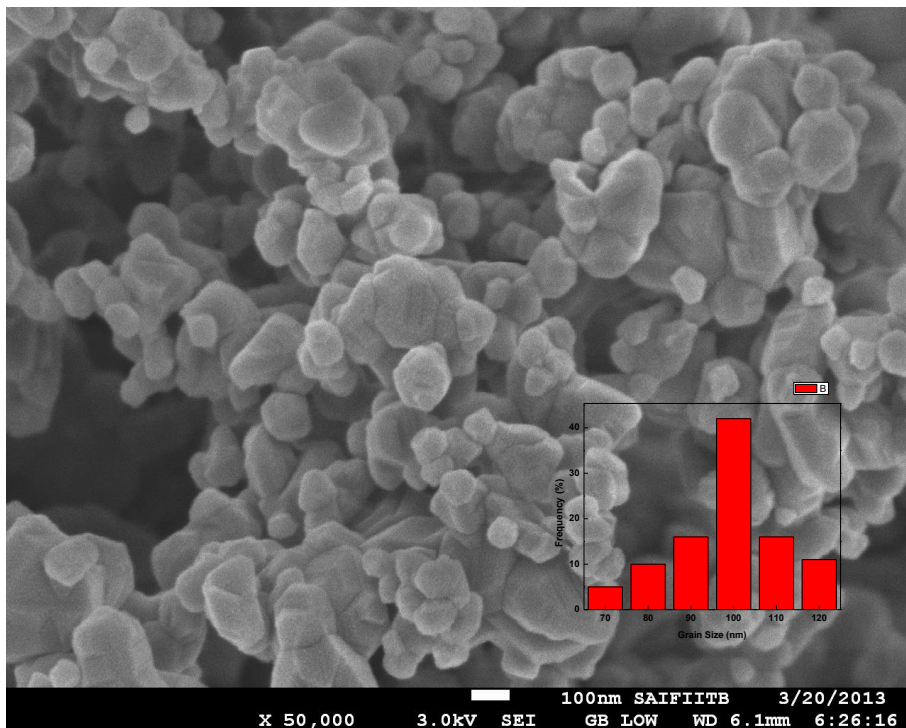
Cu Cu 1-Jun-1999 12:00 AM

Element	Weight%	Atomic%
O K	35.99	67.22
Fe K	41.35	22.13
Cu K	22.66	10.66
Totals	100.00	



EDS was performed on 6 areas and the Fe/Cu ratio was calculated as the average obtained from these 6 spectrums

3. SEM image of CuF700FC sample



4. TEM image of CuF800FC sample

